



## Design and in vitro characterization of ivermectin nanocrystals liquid formulation based on a top-down approach

Walter Javier Starkloff, Verónica Bucalá, Santiago Daniel Palma & Noelia L. Gonzalez Vidal

To cite this article: Walter Javier Starkloff, Verónica Bucalá, Santiago Daniel Palma & Noelia L. Gonzalez Vidal (2016): Design and in vitro characterization of ivermectin nanocrystals liquid formulation based on a top-down approach, Pharmaceutical Development and Technology, DOI: [10.1080/10837450.2016.1200078](https://doi.org/10.1080/10837450.2016.1200078)

To link to this article: <http://dx.doi.org/10.1080/10837450.2016.1200078>



Published online: 27 Jun 2016.



Submit your article to this journal [↗](#)



Article views: 9



View related articles [↗](#)



View Crossmark data [↗](#)

RESEARCH ARTICLE

## Design and *in vitro* characterization of ivermectin nanocrystals liquid formulation based on a top-down approach

Walter Javier Starkloff<sup>a,b</sup> , Verónica Bucalá<sup>b</sup> , Santiago Daniel Palma<sup>c</sup>  and Noelia L. Gonzalez Vidal<sup>a,d</sup> 

<sup>a</sup>Departamento de Biología, Bioquímica y Farmacia, Universidad Nacional del Sur (UNS), Bahía Blanca, Argentina; <sup>b</sup>Planta Piloto de Ingeniería Química (PLAPIQUI), UNS-CONICET, Bahía Blanca, Argentina; <sup>c</sup>Departamento de Farmacia, Facultad de Ciencias Químicas, Universidad Nacional de Córdoba, Unidad de Investigación y Desarrollo en Tecnología Farmacéutica (UNITEFA), Córdoba, Argentina; <sup>d</sup>Consejo Nacional de Investigaciones Científicas y Técnicas (CONICET), Bahía Blanca, Argentina

### ABSTRACT

The aim of this study was to develop ivermectin (IVM) nanosuspensions (NSs) to improve the dissolution rate of this poorly water-soluble drug. Different NSs combining different stabilizers, i.e. poloxamer 188 (P188), polysorbate 80 (T80), polyvinylpyrrolidone (PVP), and sodium lauryl sulfate (SLS), were prepared by high-pressure homogenization. The stabilizers were selected based on the saturation solubility and IVM stability within 72 h. The screening of formulations was performed by considering the drug content within the nanosize range. The best formulation (IVM:T80:PVP 1:0.5:0.5 wt%) was characterized in terms of the particle size distribution, morphology, crystallinity, drug content, and *in vitro* dissolution profile. This NS was also evaluated from a stability point of view, by conditioning samples at a constant temperature and relative humidity for six months. The fresh and conditioned best NSs Z-sizes were 174.6 and 215.7 nm, respectively; while both NSs showed low polydispersity indexes. The faster dissolution rate for the IVM NS was attributed to the presence of nanoparticles and changes to the crystal structure (i.e. amorphization) that further improved solubility. The best NS had a 4-fold faster initial dissolution rate than raw IVM, and is thus a promising formulation for the treatment of human and animal parasitic diseases.

### ARTICLE HISTORY

Received 12 February 2016  
Revised 9 May 2016  
Accepted 9 May 2016  
Published online 24 June 2016

### KEYWORDS

Anthelmintics; dissolution rate; high pressure homogenization; nanosuspensions; solubility; stability

### Introduction

Parasitic diseases afflict hundreds of millions of people worldwide, and are a major issue in animal health<sup>1</sup>. As most drugs available today are old and have many limitations, novel drugs or formulations for the treatment of human and animal parasitic diseases are needed<sup>2</sup>. Particularly, ivermectin (IVM) is an antiparasitic agent derived from naturally occurring fermentation products, which exhibits a broad spectrum of activity<sup>3</sup>. It is a semisynthetic derivative of the avermectins, composed of a mixture of two homologous compounds:  $\geq 80\%$  of component "a" ( $H_2B_{1a}$ ) and  $<20\%$  of component "b" ( $H_2B_{1b}$ ). IVM is an off-white nonhygroscopic crystalline powder. It has 19 asymmetric centers and is optically active. Drug stability studies have demonstrated that IVM is a stable molecule in its crystalline powdered state, but it can participate in a wide variety of reactions in acidic and basic solutions. The major uses of IVM are not only in veterinary applications to various species, but it is also an effective drug for the treatment of onchocerciasis in man<sup>4</sup>.

The aqueous solubility of IVM at room temperature is only about  $1 \mu\text{g/ml}$ . It belongs to Class II/IV in the Biopharmaceutics Classification System<sup>5</sup>. It is well-known that poorly water-soluble drugs are not easily dissolved, hence they may not be absorbed from the gastrointestinal tract sufficiently and their bioavailability may be impaired. The production of nanoparticles is one of the most promising formulation strategies to improve those properties. By reducing the particle size of a drug, the interfacial surface area, saturation solubility, and dissolution rate increase, according to the Ostwald-Freundlich and Noyes-Whitney laws<sup>6</sup>.

Nanoparticles can be obtained either by a reduction in the particle size of larger crystals (top-down approach) or by building up

particles by the precipitation of dissolved molecules (bottom-up approach)<sup>7</sup>. The bottom-up methods are not widely used due to difficulties in retaining the nanosize after precipitation, subsequent particle growth, solid-state stability, scale-up difficulties, poor drug redispersibility, residual solvent content, and high production costs<sup>8</sup>. Within the top-down techniques, high-pressure homogenization (HPH) can be regarded as one of the most important methodologies.

HPH is a scalable process, which is applied not only in the pharmaceutical but also in the cosmetics and food industries<sup>9</sup>. In addition, HPH has also been shown to overcome the drawbacks of conventional size-reducing methods such as polymorph transformation and metal contamination due to the high mechanical energy requirements associated with conventional milling processes<sup>10</sup>. Normally, a premix of the coarse drug and the dispersion medium is prepared using high-speed stirrers. The dispersion medium contains surfactant and/or stabilizer systems. Subsequently, this coarse suspension (the so-called "macro-suspension") is passed several times through the high-pressure homogenizer. Typically, the applied pressure is increased step-wise from 10% to 100% in order to avoid clogging of the narrow homogenization gap. At production pressure, the gap has an opening of only a few micrometers. Cavitation forces, shear forces, and collision cause the particle size reduction itself. In general, several homogenization cycles are needed to reach the minimal particle size<sup>11</sup>.

Drug nanocrystals are pure solid drug particles with a mean particle size below 1000 nm, ideally between 200 nm and 500 nm, with higher saturation solubility than microcrystals<sup>12</sup>. Although the term nanocrystal implies a crystalline structure, particles can be crystalline, partially crystalline, or completely amorphous. A nanosuspension

(NS) consists of drug nanocrystals, a stabilizing agent (surfactants and/or polymeric stabilizers) and a liquid dispersion medium<sup>13</sup>. The size and stability of the NS produced by top-down approaches are dependent on the solubility of the drug in the stabilizer solution<sup>14</sup>. NSs are essentially thermodynamically unstable systems. Therefore, the proper selection of stabilizers is required during the preparation of a NS in order to avoid agglomeration or crystal growth due to Ostwald ripening. The most common stabilization approaches involve steric and/or electrostatic forces. Adsorbing polymers or nonionic surfactants onto the drug particle surface achieves steric stabilization, whereas electrostatic stabilization is obtained by adsorbing charged molecules, either ionic surfactants or charged polymers, onto the particle surface. In many cases, a combination of stabilizers is required<sup>15,16</sup>.

In our research group, we have developed and optimized IVM-lipid nanocapsules intend for oral administration<sup>17</sup>. However, IVM-based nanocrystals have not been previously described. Drugs with lower aqueous solubility, higher molecular weight, and higher melting point have been shown to be good candidates for NS production (i.e. easier to stabilize)<sup>15,18</sup>. IVM has a molecular weight between 872.21 and 875.10 g/mol (depending on the relative fraction of components H<sub>2</sub>B<sub>1a</sub> and H<sub>2</sub>B<sub>1b</sub>) and a melting point of 155 °C<sup>4</sup>. Thus, it is a good drug candidate to be administered as a NS.

This study aimed to develop a physicochemically stable NS able to improve the dissolution behavior of IVM. After screening a number of stabilizing agents, based on the study of IVM saturation solubility, different NSs were produced by the HPH method. The NSs were characterized in terms of particle size distribution, morphology, crystallinity, drug content and *in vitro* dissolution profiles, and compared with the properties exhibited by the starting materials, i.e. raw IVM and a physical mixture of the drug with the selected stabilizers. The stability of the best NS was also evaluated. The development of an optimized formulation, capable of improving the unfavorable dissolution properties of this drug, could be a promising option for the treatment of human and animal parasitic diseases.

## Materials and methods

### Materials

Pharmaceutical grade IVM (Todo Droga, Córdoba, Argentina), which complied with the European Pharmacopoeia 5.0<sup>19</sup> requirements, was used. Pharmaceutical-grade poloxamer 188 (P188 – Lutrol F68<sup>®</sup>), polyvinylpyrrolidone K30 (PVP – BASF), and polysorbate 80 (T80 – Tween 80<sup>®</sup>) were purchased from Droguería Saporiti (C.A.B.A., Argentina). Sodium lauryl sulfate (SLS) was acquired from Laboratorios Cicarelli (San Lorenzo, Argentina). Triple distilled water was used for the formulation of NSs. HPLC grade methanol, acetonitrile, and water were purchased from Sintorgan (Villa Martelli, Argentina). Potassium dihydrogen phosphate (Anedra -Research AG- Tigre, Argentina) and sodium hydroxide (Cicarelli, San Lorenzo, Argentina), analytical grade, and deionized water were used for the dissolution media preparation. For particle size analysis, ultrapurified Milli-Q<sup>®</sup> water (Millipore SAS, Molsheim, France) was used for dilution.

### Methods

#### Raw IVM saturation solubility

In order to prepare the initial dispersions for HPH process, the saturation solubility is required to establish the IVM content that ensures supersaturation conditions. For this reason, the solubility of IVM (as supplied) was determined in different stabilizer

solutions, and compared with the drug solubility in triple distilled water and phosphate buffer (pH 5.8). This pH value was selected to emulate ruminal acidity, considering the potential application of the formulated NSs to the treatment of ruminants. Another critical parameter in nanocrystal production is the process temperature, which strongly affects drug solubility<sup>12</sup>. Since the HPH increased the dispersion temperature, as discussed below, the process was controlled in order to not exceed 40 °C. For this reason, the saturation solubility tests were performed at this temperature.

The stabilizer solutions were prepared by mixing ionic or non-ionic surfactants (SLS or T80, respectively) with a polymeric stabilizer (PVP or P188) to form binary mixtures at a 1:1 ratio and a total concentration of 1% or 2% (w/v) in triple distilled water. An excess of drug and 7 ml of each stabilizer solution were added to screw-capped tubes. The solubility experiment was performed at 40 °C. To this end, the tubes were immersed in a shaking water bath (Gerhardt Schüttelwasserbad SW 20, Germany), thermostatically controlled for 72 h (at this time, the equilibrium was reached for all the stabilizer solutions). Each sample was centrifuged (3500 rpm, 30 min) using a Rolco CM 2036 (Liniers, Argentina), and the supernatant was filtered through 0.45- $\mu$ m pore nylon membrane (Microclar, Tigre, Argentina). An aliquot was evaluated by UV-spectrophotometry (Varian Cary 50Conc, Varian Instruments, Mulgrave, Australia), at the maximum IVM absorption wavelength, i.e. 245 nm<sup>4</sup>. No interference from the stabilizer solutions was detected under the same analytical conditions. Each sample was analyzed in triplicate.

#### NSs preparation

To prevent blockage of the homogenization valve in the HPH process, pre-milling of the suspension is required. Coarse drug suspensions were prepared by dispersing IVM (as supplied) in different stabilizer solutions. The IVM:stabilizers ratio was 1:1 (w/w). IVM was gently wetted with the stabilizer solution in a glass mortar. The suspensions were mixed using a magnetic stirrer at 1000 rpm for 5 min, and sonicated for 10 min at maximum power using an ultrasonic bath (Testlab TB018TDCD, Bernal Oeste, Argentina). The bath medium was a mixture of water and 0.2% (w/v) SLS in order to increase cavitation forces. The obtained coarse suspensions were then homogenized at high pressure (40 cycles at 800 bar) using an APV 1000 apparatus (Soeborg, Denmark). Due to the high input of energy, the outlet stream (i.e. recycled for further homogenization) exhibited temperature increases. In order to control the processing temperature, four cycles under pressure were followed by 10 cycles without pressure, and the suspension to be recycled was cooled down each time by its circulation through a water bath maintained at 20 °C. By doing this, the suspension temperature was controlled in order to not exceed 40 °C.

#### Physical mixture preparation

Physical mixtures (PM) were prepared by blending IVM and the stabilizers in a glass mortar until a homogeneous mixture was obtained. For this purpose, the same drug/stabilizer ratios (w/w) as the IVM NSs were used.

#### Particle size analysis

The mean hydrodynamic radius (Z-size) and polydispersity index (PI) of the nanoparticles were determined by photon correlation spectroscopy (PCS) using a Zetasizer Nano ZS90 (Malvern Instruments, Worcestershire, UK). Samples were backscattered by a helium-neon laser (633 nm) at an angle of 90°, and a constant temperature of 25 °C. Each sample was analyzed immediately after

its formulation, in triplicate. In order to avoid concentration-dependent effects (i.e. particle interactions), the sample was suitably diluted using ultrapurified water until the results were independent of the particle concentration.

The measurable range of the Zetasizer is approximately 2 nm to 3  $\mu\text{m}$ . Thus, laser diffraction (LD; HORIBA LA950-V2, Kyoto, Japan), with a measuring range up to 2000  $\mu\text{m}$ , was employed to observe larger particles. The raw IVM was characterized by LD, using the unit equipped with a powder jet dry feeder system at 0.2 MPa airflow. Measurements were performed in triplicate, and volumetric particle size distributions were obtained. LD results were expressed in terms of the mean diameter over volume ( $D_{43}$ ) and its corresponding standard deviation (SD).

#### Powder X-ray diffraction analysis

Powder X-ray diffraction analysis (PXRD) patterns of the raw materials, PM, and NSs were recorded with a Rigaku D/Max IIC (Tokyo, Japan) diffractometer with a Ni-filtered  $\text{CuK}_\alpha$  radiation detector ( $\lambda = 1.5405 \text{ \AA}$ ), operating at a voltage of 35 kV and a current of 15 mA in the  $2\theta$  range from  $2.5^\circ$  to  $60^\circ$ , with a scan angular speed of  $2^\circ/\text{min}$  and a scan step of  $0.02^\circ$ . In the case of T80, PXRD analysis was not performed because the material is in the liquid state at room temperature. For the analysis of IVM NS, the liquid formulation was dried in a thermostatically controlled oven at  $40^\circ\text{C}$  in order to obtain a dried powder.

A computer program (MDI/JADE7, Jacksonville, FL) involving the use of self-modelling curve resolution (SMCR) and multivariate curve resolution (MCR) methods was employed to analyze the X-ray diffraction data and to study the interactions between IVM and stabilizers in the NS.

#### Differential scanning calorimetry

Thermal analysis was performed using a Perkin Elmer Pyris1 (Perkin Elmer, Waltham, MA). The instrument was calibrated with indium (calibration standard, purity 99.999%) for melting point and heat of fusion. About 9 mg of raw IVM, PVP, and dried NS samples were scanned from 25 to  $200^\circ\text{C}$ , at a heating rate of  $10^\circ\text{C}/\text{min}$  in aluminum-crippled pans under nitrogen gas flow. An empty aluminum pan was used as the standard reference. In the case of T80, the material is in liquid state at room temperature and has a flash point of  $149^\circ\text{C}$ <sup>20</sup>. Therefore, at temperatures that are representative of IVM thermal events (i.e. IVM melting point:  $169.7^\circ\text{C}$ ), differential scanning calorimetry (DSC) analysis of raw T80 and PM was unfeasible. Nevertheless, in the NS, T80 is attached to the nanoparticles and trapped by PVP chains, and thus behaves with completely different identity with respect to the raw materials. It was thus possible to perform the DSC test.

The purpose of the first thermal scan was to remove the residual moisture that could affect the determination of  $T_g$ . Then, the samples were cooled from  $200$  to  $25^\circ\text{C}$ , at a cooling rate of  $10^\circ\text{C}/\text{min}$ , and reheated from  $20$  to  $200^\circ\text{C}$  at the same rate.  $T_g$  was calculated from thermograms as the temperature at which one-half of the change in heat capacity,  $\Delta C_p$ , occurred (i.e. the half  $\Delta C_p$  method)<sup>21</sup>.

#### Particle morphology evaluation

The morphology of IVM particles in the NSs, PM, and bulk drug were examined by Scanning Electronic Microscopy (SEM; LEO EVO 40-XVP, Oberkochen, Germany). A drop of fresh NS was dispersed onto glasses coverslips, and the water was left to evaporate naturally. The obtained powder was fixed on aluminum stubs using doubled-sided adhesive tape and coated with Au in a sputter coater (PELCO 91000, Redding, CA).

#### High performance liquid chromatography analysis

An isocratic high performance liquid chromatography (HPLC) method was employed for the quantification of IVM<sup>22</sup>, in dissolution and stability studies, and to probe for the presence of IVM degradation products in saturated solutions containing SLS. A Spectra System (Thermo, San Jose, CA) equipped with a P4000 pump unit, an SCM1000 degasifier, an injection valve with a simple loop of 20  $\mu\text{l}$  volume (Rheodyne 9125), and an Ultrasphere C18 column ( $4.6 \times 250 \text{ mm}$ ,  $5 \mu\text{m}$ ; Beckman, Atlanta, GA) was used. The column was maintained at room temperature. The mobile phase consisted of a mixture of acetonitrile:methanol:water (51:34:15). The flow rate was 1.0 ml/min, and the UV detector (UV2000, Spectra System, Thermo, San Jose, CA) was set at 245 nm.  $\text{H}_2\text{B}_{1a}$  eluted at 18.6 min and  $\text{H}_2\text{B}_{1b}$  at 14.5 min, under the conditions described above. An external standard calibration curve was established by using solutions of IVM in methanol within the range of 0.0058–0.58 mg/ml, with a  $R^2$  value of 0.9999, referring to component  $\text{H}_2\text{B}_{1a}$ .

#### In vitro dissolution studies

*In vitro* dissolution studies were performed using the paddle method, at a rotation speed of 50 rpm (Erweka DT60, Heusenstamm, Alemania). The dissolution medium was 900 ml of phosphate buffer (pH 5.8), prepared according USP 30<sup>23</sup>, with 0.5% (w/v) SLS, kept at  $37.0 \pm 0.5^\circ\text{C}$ . The pH of the dissolution medium, as mentioned above, was selected to emulate ruminal acidity. SLS was added to enhance the dissolution rate of IVM, considering the ability of surfactants to accelerate this process, due to a reduction in the interfacial tension and micellar solubilization properties<sup>24</sup>.

Samples (10 ml) were withdrawn at 7, 15, 30, and 45 min (an equal volume of pre-warmed fresh dissolution medium was replaced after each extraction) and immediately filtered through a  $0.22\text{-}\mu\text{m}$  pore nylon membrane (Gamafil, Béccar, Argentina). The amount of IVM dissolved was determined by HPLC, and the mean results and standard deviation were reported. To provide the same drug amount, dissolution tests were performed, in triplicate, using 10 ml of NSs, 100 mg of IVM bulk drug, and 200 mg of IVM-stabilizer PM.

#### Stability studies

Drug stability studies were performed to assess the stability of IVM NS, under controlled conditions of temperature and relative humidity ( $25 \pm 2^\circ\text{C}$ ,  $60 \pm 5\% \text{ RH}$ ) for a period of six months. NS was stored in closed vials, protected from light, in a pharmaceutical stability chamber (SCT Pharma ICH 830 L, Temperley, Argentina). After conditioning, the NS particle size distribution, drug content, morphology of nanocrystals, crystallinity, and *in vitro* dissolution rate were evaluated.

#### Statistical analysis

Analysis of variance (ANOVA) was performed using InfoStat<sup>25</sup>. Multiple comparisons were achieved by Fisher's LSD test. Results are expressed as mean  $\pm$  standard deviation of replicate analyses. Differences with  $p$  values less than 0.05 ( $p < 0.05$ ) were considered statistically significant.

## Results and discussion

#### Raw IVM saturation solubility and NSs formulation

Figure 1 shows the IVM saturation solubility in different media at  $40^\circ\text{C}$ . The IVM solubility, as expected, was very low in phosphate buffer (pH 5.8) and in triple distilled water. The mixtures

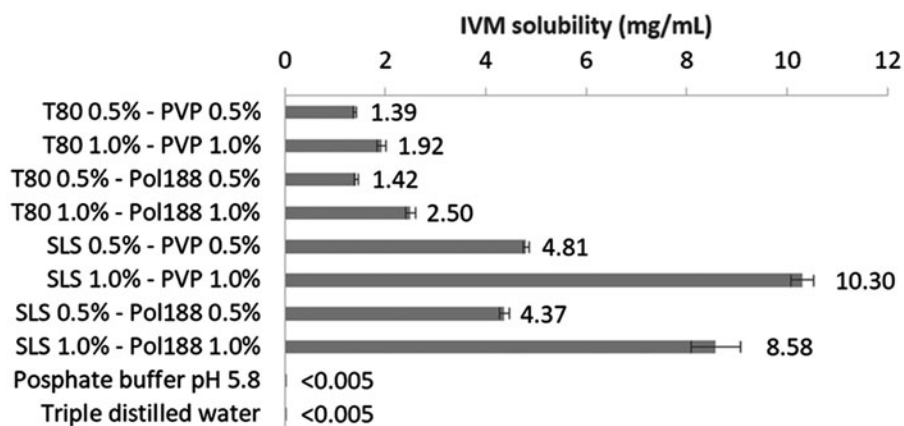


Figure 1. Ivermectin solubility in different media and at 40 °C. Stabilizers concentration expressed as % w/v.

containing SLS, even though using different stabilizer amounts, had the apparent highest saturation solubility. However, the dispersions containing SLS exhibited a yellowish appearance after 48 h at the selected temperature. For this reason, after centrifugation, the filtered supernatant of the sample containing SLS was analyzed by HPLC. Figure 2(a,b) show the HPLC chromatograms for pure IVM dissolved in methanol and the filtered supernatant of the sample containing SLS (0.5% w/v) and PVP (0.5% w/v), respectively. In both cases, the same IVM final concentration was injected (0.31 mg/ml). Figure 2(a) shows two peaks that eluted at 15.8 and 20.5 min, which are related to the components  $H_2B_{1b}$  and  $H_2B_{1a}$ , respectively. The relative retention times ( $H_2B_{1a}$  to  $H_2B_{1b}$ ) were about 1.3, a value that is in good agreement with the USP 30 Monograph for IVM<sup>23</sup>. The HPLC chromatogram for the sample containing SLS (Figure 2(b)) showed a reduction in the area of the  $H_2B_{1b}$  and  $H_2B_{1a}$  peaks, and the occurrence of secondary peaks, indicating IVM degradation. Because IVM contains many functional groups, it can participate in a wide variety of reactions in acidic and basic solutions. Besides, IVM is subject to oxidative degradation, which occurs preferably in aqueous surfactant solutions<sup>4</sup>. These results indicate that SLS did not behave as an adequate stabilizer for the formulation of an IVM NS.

On the other hand, nonionic surfactants, like T80, are described as pharmaceutically acceptable and compatible with IVM, with regard to solubility and chemical stability<sup>26</sup>. The presence of T80, combined with either PVP or P188, substantially increased IVM solubility, with respect to IVM solubility in triple distilled water (Figure 1). In addition, these dispersions did not exhibit color changes. For these reasons, these stabilizers were used to prepare the NSs. An IVM concentration of 10 mg/ml (i.e. 1% w/v) was selected to ensure supersaturation conditions (Figure 1). Additionally, an IVM:stabilizers ratio of 1:1 was selected for the formulation of NSs, because doubling the total stabilizer content does not double the solubility.

T80 has been found to be useful in improving the oral bioavailability of drug molecules that are substrates for p-glycoprotein (P-gp)<sup>27</sup>. In addition, it has been observed that apical-to-basolateral transport of certain drugs across Caco-2 monolayers is enhanced at pharmaceutically relevant concentrations of T80, namely those that are substrates of P-gp or MRP-like efflux systems<sup>28</sup>. Several authors have reported evidence that a broad variety of nonionic surfactants have an inhibitory effect not only on P-gp but also on other ABC transporters, such as BCRP and MRPs<sup>29-31</sup>. This evidence is relevant because IVM has been reported to be a substrate of P-gp<sup>32</sup>, and can induce the overexpression of P-gp, thereby reducing its effectiveness and increasing resistance<sup>33</sup>. Thus, a NS containing T80 could be an advantageous formulation.

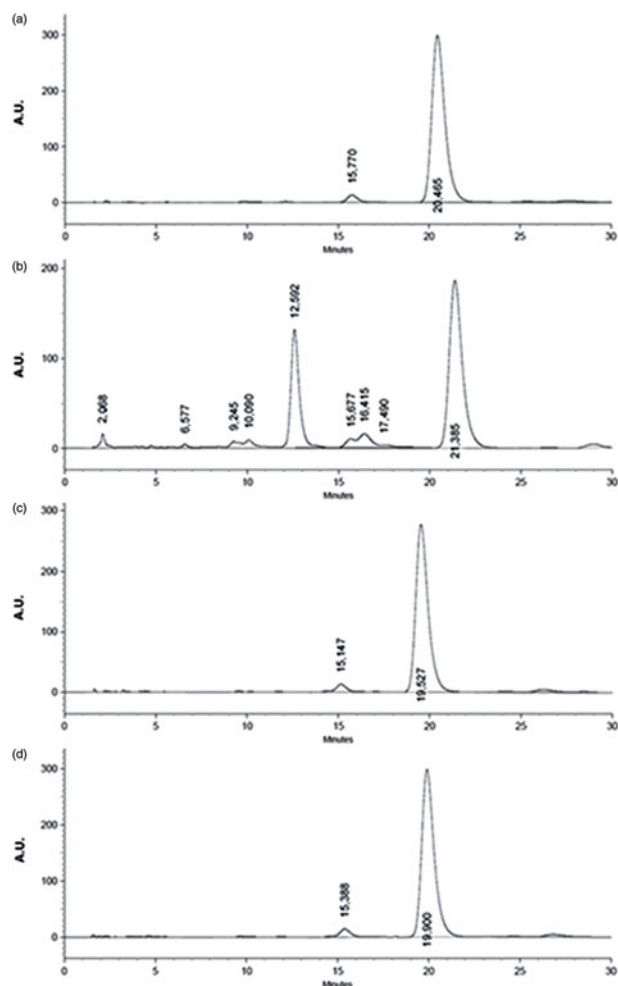


Figure 2. HPLC results: IVM solution (solvent: methanol) (a), IVM + SLS (0.5% w/v) + PVP (0.5% w/v) (b), fresh NS1 (c), and NS1 after six months of storage (d). A.U.: Arbitrary units.

Finally, a recovery study was performed to select the best stabilizing polymeric agent. For this reason, NSs formulated with T80, in the presence of PVP or P188, were filtered through a 0.45- $\mu$ m pore nylon membrane filter. The filtered NSs were dissolved in ethanol and quantified by UV-spectrophotometry (as described in the

**Table 1.** Size parameters obtained by LD and PCS.

LD	D <sub>43</sub> (μm)	SD (μm)	D <sub>10</sub> (μm)	D <sub>50</sub> (μm)	D <sub>90</sub> (μm)
Bulk IVM	220.7 ± 13.1	159.1 ± 17.2	44.0 ± 2.2	192.8 ± 9.2	434.4 ± 34.1
PCS	Z-size (nm)	PI	D <sub>50</sub> (nm)	D <sub>90</sub> (nm)	D <sub>95</sub> (nm)
Fresh NS1	174.6 ± 2.1	0.357 ± 0.036	236 ± 5	324 ± 49	357 ± 50
NS1 after six months of storage	215.7 ± 1.6 <sup>a</sup>	0.204 ± 0.001 <sup>a</sup>	240 ± 7 <sup>ns</sup>	357 ± 35 <sup>ns</sup>	394 ± 45 <sup>ns</sup>

<sup>a</sup>High significant differences ( $p < 0.001$ ); <sup>ns</sup>No significant differences.

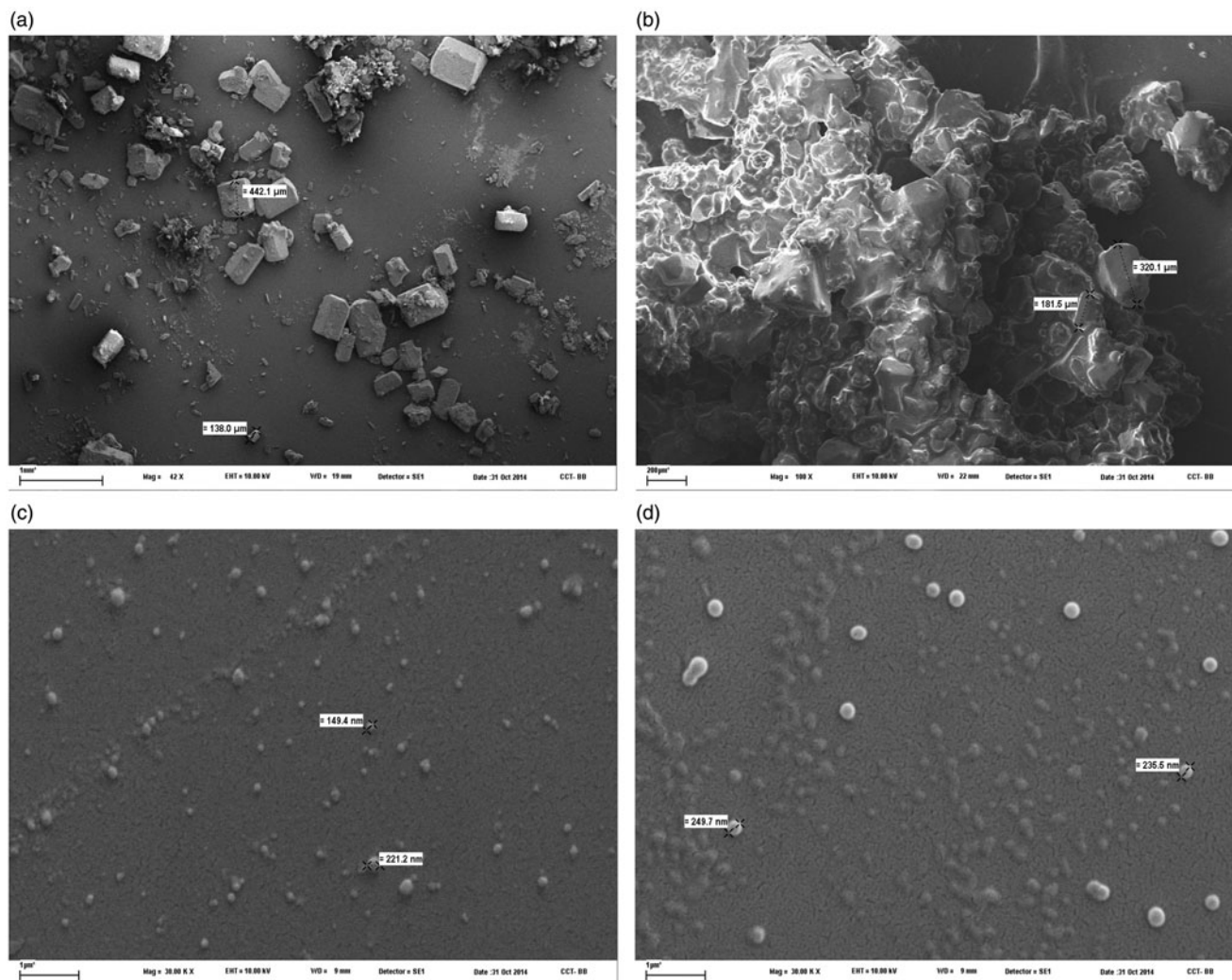


**Figure 3.** SEM micrographs of raw IVM (a), physical mixture (b), fresh NS 1 (c), and NS 1 after six months of storage (d).

section "Raw IVM saturation solubility"). IVM NS formulated with T80-PVP showed an IVM recovery of 52% in the filtered liquid (i.e. dissolved IVM + IVM nanoparticles), while a value of 19% was measured for T80-P188 (data not shown).

According to the described results, the NS formulated at an IVM concentration of 1% (w/v) with a stabilizing solution of T80 (0.5% w/v) – PVP (0.5% w/v) was selected as the model formulation (NS1). The stabilization efficiency of these agents could be explained by the results described by Cabane and Nakach et al., which explain the specific interaction between hydrosoluble polymers and surfactants. Both authors have described their results as a synergistic combination of stabilizers. As in pure surfactant micelles, the lipophilic chains of the surfactant molecules appear to be gathered in the hydrophobic core of the active pharmaceutical ingredient, while their polar groups are spread on the interface, interacting with monomers of the polymer chain<sup>34,35</sup>.

### Particle size measurement

As shown in Table 1, the average mean particle size ( $n = 3$ ) for raw IVM was approximately 221 μm. HPH of IVM dispersions produced a significant reduction in the particle size of the bulk drug, since the Z-size obtained for fresh NS1 was about 150.4 nm, with a PI value of 0.521. IVM nanoparticles exhibited a mean particle size approximately three orders of magnitude lower than the one corresponding to raw IVM. A narrow particle size distribution avoids problems with the variable saturation solubility of particles with different sizes, thus inhibiting Ostwald ripening and providing long-term stability<sup>36</sup>.

### Morphology evaluation

The SEM micrographs of the raw material, PM, and NS1 are shown in Figure 3. Raw IVM showed an irregular shape, with particles

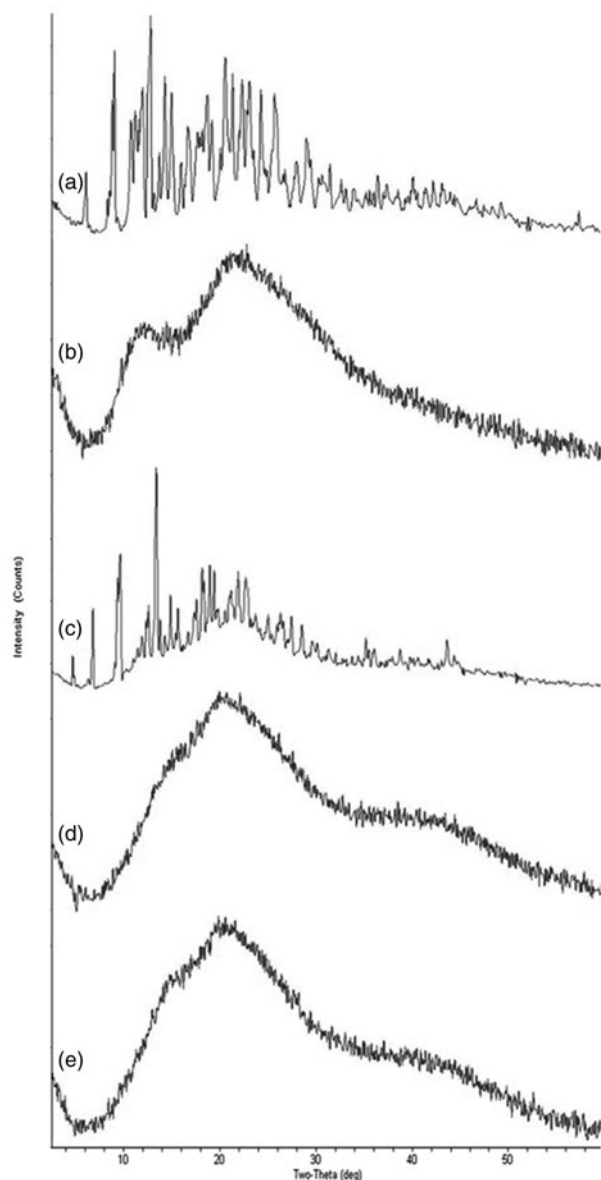


**Figure 4.** X-ray diffractograms for raw IVM (a), raw PVP (b), physical mixture (c), fresh NS 1 (d), and NS 1 after six months of storage (e).

larger than 450  $\mu\text{m}$  (Figure 3(a)). Figure 3(b) shows the PM, which was an agglomerate containing large IVM particles. The nanoparticles were mainly spheres, and their sizes were in good agreement with those derived from PCS (Figure 3(c); Table 1). In addition to the particle size distribution analysis, the SEM micrographs provide further evidence that HPH resulted in significant reduction in particle size. It is evident that the size of the IVM nanoparticles was significantly smaller and the shape was more homogeneous than in the raw material, properties that could be beneficial in terms of enhancing bioavailability.

#### Solid state evaluation and crystallinity

The assessment of the crystalline state helps in understanding molecular interactions in the solid state. PXRD was performed to investigate the effect of the HPH process on the crystallinity of IVM. As shown in Figure 4(a), the pattern of the raw IVM exhibited some intense crystalline peaks between 6° and 22° of 2 $\theta$ , which prove that

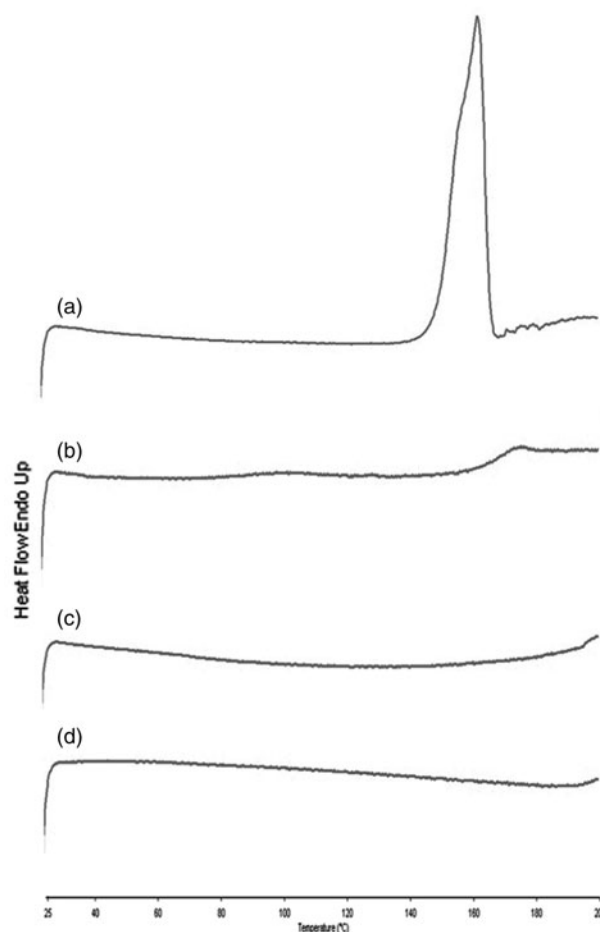


**Figure 5.** DSC thermograms of IVM raw material (a), PVP raw material (b), fresh NS1 (c), and NS1 after six months of storage (d).

the raw material was crystalline. Even though PVP is amorphous (Figure 4(b)), the PM showed peaks that can be related to the crystalline structure of IVM (Figure 4(c)). Only one broad and diffuse maximum peak was detected in the PXRD patterns of fresh NS1 (Figure 4(d)), which indicated that the nanosized IVM was amorphous.

#### Thermal analysis

As shown in Figure 5(a), the thermal behavior of raw IVM showed an onset temperature of 149.3°C and a melting peak at 161.7°C, in agreement with the results given by Fink<sup>4</sup>. PVP K30 showed a glass transition temperature close to 166°C (Figure 5(b)), a similar value to the one obtained by Turner and Schwartz for the second heating of PVP K-30 samples<sup>37</sup>. The NS1 thermogram did not exhibit significant thermal events (Figure 5(c)), which confirms the disappearance of crystallinity as indicated by PXRD.

#### IVM dissolution

Figure 6 presents the dissolution profiles of raw IVM, PM, and NS1. The dissolution rates can be inferred from this figure as the local slope of these profiles. Pure IVM presented a low initial dissolution rate, and after 45 min only 64% was dissolved. The PM, with an even lower initial dissolution rate, reached almost the same total dissolution as raw IVM. In contrast, NS1 exhibited a significant higher

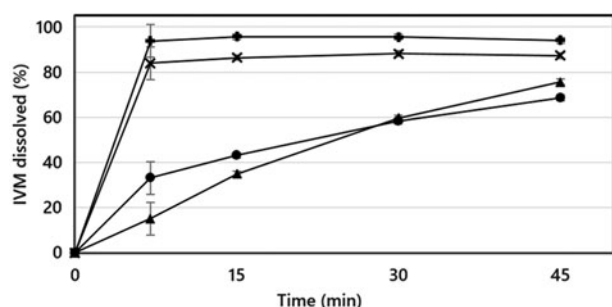


**Figure 6.** Dissolution profiles of raw IVM (●), physical mixture (▲), fresh NS1 (+), and conditioned NS1 (×).

dissolution rate than PM and raw IVM. For NS1, more than 80% of the drug was dissolved in the first 7 min compared to 15% for raw IVM and less than 45% for PM. ANOVA analysis indicated that dissolved percentages at 7 min, between raw IVM and NS1, were statistically different ( $p < 0.001$ ). The formulation of IVM as a NS was very successful in enhancing the dissolution rate, which may increase the concentration of IVM in the gastrointestinal lumen, and hence improve the treatment of enteric parasitic diseases.

The rapid IVM dissolution observed for NS1 can be attributed to the presence of nanoparticles and changes in the crystal structure (i.e. amorphization) that further improved solubility<sup>38,39</sup>. Both formulation characteristics were caused by the high energy forces applied during the homogenization process. The increase in the surface-to-volume ratio, due to the submicron dimension of the drug particles, improved the NS dissolution rate, as predicted by the Noyes–Whitney model<sup>40–43</sup>.

### NS1 stability

During the stability study of the formulation, shape changes were not detected (Figure 3(d)). ANOVA of the particle size measurements showed statistically significant differences in Z-size and PI between fresh NS1 and NS1 after 6 months, while their cumulative distributions showed no differences (Table 1). Nevertheless, NS1 after 6 months of storage still presented a Z-size in the nanometric range (215.8 nm) and a PI value below 0.3, indicating a narrow particle size distribution<sup>44</sup>. Distributions with low PI values inhibit the occurrence of Ostwald ripening<sup>7,44,45</sup>. This can explain why Ostwald ripening is not a major concern for NS1 with a uniform particle size. Similar PXRD patterns were observed after six months of storage, indicating that the nanoparticles remained amorphous (Figure 4(e)). These results are in good agreement with those derived from DSC (Figure 5(d)). As shown in Figure 6, the amount of IVM dissolved at 7 min from the conditioned NS1 was approximately 4-fold higher than IVM dissolved from the PM. Nevertheless, the analyzed formulation exhibited an initial dissolution rate slightly slower than that of fresh NS1, but with no statistically significant differences observed (up to 7 min). Finally, the HPLC chromatograms showed characteristic IVM peaks, not only for fresh NS1 but also for NS after six months of storage, suggesting no IVM degradation (Figure 2(c,d)). Therefore, all the performed tests indicated remarkable stability of NS1.

### Conclusions

A NS formulation of IVM, containing T80 and PVP as stabilizers, was developed. The IVM nanoparticles produced by the HPH method were amorphous with a narrow PI, and chemically stable.

The dissolution of nanosized IVM was significantly enhanced with respect to the performance exhibited by the raw material or PM. In conclusion, the HPH method offers a simple and robust process to obtain nanoparticles of adequate size and stability, and provides a significant improvement in the dissolution rate of IVM.

By definition, BCS Class II drugs, such as IVM, exhibit bioavailability problems directly related to their solubility and dissolution rate in physiological fluids. Moreover, IVM is a P-gp substrate, so it can be assigned to BCS Class IV. The developed NS would overcome these two obstacles by the reduction in particle size and the incorporation of T80 as a stabilizer, which increase the dissolution rate and inhibit P-gp, respectively. Therefore, NS1 is a promising formulation for improvement of antiparasitic chemotherapy.

### Acknowledgements

The authors kindly thank Graciela Mas (Universidad Nacional del Sur, CONICET), Fernanda Cabrera (CONICET), and María Julia Yañez (CONICET) for their technical assistance with X-ray diffraction, DSC, and SEM analyses, respectively. The authors would like to thank Vanessa Fetter for collaboration with dissolution studies.

### Disclosure statement

The authors report no declarations of interest.

### Funding information

Walter J. Starkloff is a doctoral fellowship holder of Consejo Nacional de Investigaciones Científicas y Técnicas (CONICET, Argentina). This work was supported by Universidad Nacional del Sur (PGI 24/ZB56) and CONICET (PIP CONICET 112 201101 00336).

### ORCID

Walter Javier Starkloff <http://orcid.org/0000-0002-5111-4353>  
 Verónica Bucalá <http://orcid.org/0000-0002-5707-4436>  
 Santiago Daniel Palma <http://orcid.org/0000-0003-4468-1111>  
 Noelia L. Gonzalez Vidal <http://orcid.org/0000-0002-0687-0096>

### References

1. Torgerson PR, Macpherson CNL. The socioeconomic burden of parasitic zoonoses: global trends. *Vet Parasitol* 2011; 182:79–95.
2. Rohwer A, Marhöfer RJ, Caffrey CR, Selzer PM. Drug discovery approaches toward anti-parasitic agents. In: Becker K, ed. *Apicomplexan parasites: molecular approaches toward targeted drug development*. Weinheim: Wiley-VCH Verlag GmbH & Co. KGaA; 2011:3–20.
3. Ōmura S, Crump A. Ivermectin: panacea for resource-poor communities? *Trends Parasitol* 2014;30:445–455.
4. Fink DW. Ivermectin. In: Florey K, ed. *Analytical profiles of drug substances*. New York: Academic Press; 1988:155–184.
5. WHO Technical Report Series No. 937 Annex 8. Proposal to waive in vivo bioequivalence requirements for WHO Model List of Essential Medicines immediate-release solid oral dosage forms. Geneva: World Health Organization; 2006.
6. Müller RH, Jacobs C, Kayser O. Nanosuspensions as particulate drug formulations in therapy. Rationale for development and what we can expect for the future. *Adv Drug Deliv Rev* 2001;47:3–19.



7. Rabinow BE. Nanosuspensions in drug delivery. *Nat Rev Drug Discov* 2004;3:785–796.
8. Hu J, Ng WK, Dong Y, et al. Continuous and scalable process for water-redispersible nanoformulation of poorly aqueous soluble APIs by antisolvent precipitation and spray-drying. *Int J Pharm* 2011;404:198–204.
9. Dumay E, Chevalier-Lucia D, Picart-Palmade L, et al. Technological aspects and potential applications of (ultra) high-pressure homogenization. *Trends Food Sci Technol* 2013;31:13–26.
10. Kluge J, Muhrer G, Mazzotti M. High pressure homogenization of pharmaceutical solids. *J Supercrit Fluids* 2012;66:380–388.
11. Möschwitzer JP. Drug nanocrystals in the commercial pharmaceutical development process. *Int J Pharm* 2013;453:142–156.
12. Keck CM, Müller RH. Drug nanocrystals of poorly soluble drugs produced by high pressure homogenization. *Eur J Pharm Biopharm* 2006;62:3–16.
13. Ige PP, Baria RK, Gattani SG. Fabrication of fenofibrate nanocrystals by probe sonication method for enhancement of dissolution rate and oral bioavailability. *Colloids Surf B Biointerfaces* 2013;108:366–373.
14. Verma S, Lan Y, Gokhale R, Burgess DJ. Quality by design approach to understand the process of nanosuspension preparation. *Int J Pharm* 2009;377:185–198.
15. Van Eerdenbrugh B, Van den Mooter G, Augustijns P. Top-down production of drug nanocrystals: nanosuspension stabilization, miniaturization and transformation into solid products. *Int J Pharm* 2008;364:64–75.
16. Bilgili E, Li M, Afolabi A. Is the combination of cellulosic polymers and anionic surfactants a good strategy for ensuring physical stability of BCS Class II drug nanosuspensions? *Pharm Dev Technol* 2016;21:499–510.
17. Ullio Gamboa G, Llolo G, Benoit J, et al. Development and optimization of ivermectin-lipid nanocapsules intend for oral administration. Conference Proceeding – 3rd International Meeting on Pharmaceutical Sciences, Córdoba, Argentina, 2014.
18. Wu L, Zhang J, Watanabe W. Physical and chemical stability of drug nanoparticles. *Adv Drug Deliv Rev* 2011;63:456–469.
19. European Pharmacopoeia, 5th ed. Main Volume 5.0. Council of Europe. Strasbourg, France; 2005:1854–1856.
20. Zhang D. Polyoxyethylene sorbitan fatty acid esters. In: Rowe RC, Sheskey PJ, Quinn ME, eds. *Handbook of pharmaceutical excipients*. 6th ed. London–Chicago: Pharmaceutical Press and the American Pharmacists Association; 2009:549–553.
21. Shrestha AK, Howes T, Adhikari AK, Bhandari B. Water sorption and glass transition properties of spray dried lactose hydrolyzed skim milk powder. *LWT Food Sci Tech* 2007;40:1593–1600.
22. Farmacopea Nacional Argentina, Séptima Edición. Volumen 2, Monografía de Materia Prima, Ivermectina: Valoración. ANMAT, Buenos Aires, Argentina, 2013.
23. The United States Pharmacopoeia and National Formulary, USP 30-NF 25. Spanish Edition. Rockville, MD: The United States Pharmacopoeial Convention, Inc.; 2007:1362–1363.
24. Shah VP, Konecny JJ, Everett RL, et al. In vitro dissolution profile of water-insoluble drug dosage forms in the presence of surfactants. *Pharm Res* 1989;6:612–618.
25. Di Rienzo JA, Casanoves F, Balzarini MG, et al. InfoStat 2014 version. Grupo InfoStat, FCA, Universidad Nacional de Córdoba, Argentina. Available from: <http://www.infostat.com.ar>.
26. Guzzo CA, Clineschmidt CM, Schorn G, Reynolds JM. Inventors. Topical ivermectin composition. US patent 7064108 B2. June 20; 2006. Available from: <http://www.google.com/patents/US7064108>.
27. Nerurkar MM, Burton PS, Borchardt RT. The use of surfactants to enhance the permeability of peptides through Caco-2 cells by inhibition of an apically polarized efflux system. *Pharm Res* 1996;13:528–534.
28. Rege BD, Yu LX, Hussain AS, Polli JE. Effect of common excipients on Caco-2 transport of low-permeability drugs. *J Pharm Sci* 2001;90:1776–1786.
29. Cuestas ML, Sosnik A, Mathet VL. Poloxamines display a multiple inhibitory activity of ATP-binding cassette (ABC) transporters in cancer cell lines. *Mol Pharm* 2011;8:1152–1164.
30. Guo S, Zhang X, Gan L, et al. Effect of poly (ethylene oxide)-poly (propylene oxide)-poly (ethylene oxide) micelles on pharmacokinetics and intestinal toxicity of irinotecan hydrochloride: potential involvement of breast cancer resistance protein (ABCG2). *J Pharm Pharmacol* 2010;62:973–984.
31. Yamagata T, Morishita M, Kusuhara H, et al. Characterization of the inhibition of breast cancer resistance protein-mediated efflux of mitoxantrone by pharmaceutical excipients. *Int J Pharm* 2009;370:216–219.
32. Didier A, Loor F. The abamectin derivative ivermectin is a potent P-glycoprotein inhibitor. *Anticancer Drugs* 1996;7:745–751.
33. Menez C, Mselli-Lakhal L, Foucaud-Vignault M, et al. Ivermectin induces P-glycoprotein expression and function through mRNA stabilization in murine hepatocyte cell line. *Biochem Pharmacol* 2012;83:269–278.
34. Cabane B. Structure of some polymer-detergent aggregates in water. *J Phys Chem* 1977;81:1639–1645.
35. Nakach M, Authelin J-R, Tadros T, et al. Engineering of nanocrystalline drug suspensions: employing a physico-chemistry based stabilizer selection methodology or approach. *Int J Pharm* 2014;476:277–288.
36. Gao L, Zhang D, Chen M. Drug nanocrystals for the formulation of poorly soluble drugs and its application as a potential drug delivery system. *J Nanoparticle Res* 2008;10:845–862.
37. Turner DT, Schwartz A. The glass transition temperature of poly(N-vinyl pyrrolidone) by differential scanning calorimetry. *Polymer* 1985;26:757–762.
38. Müller RH, Jacobs C, Kayser O. DissoCubes—a novel formulation for poorly soluble and poorly bioavailable drugs. In: Nielloud F, Marti-Mestres G, eds. *Pharmaceutical emulsions and suspensions*. New York: Marcel Decker; 2003:383–407.
39. Van Eerdenbrugh B, Vermant J, Martens JA, et al. Solubility increases associated with crystalline drug nanoparticles: methodologies and significance. *Mol Pharm* 2010;7:1858–1870.
40. Noyes AA, Whitney WR. The rate of solutions of solid substances in their own solutions. *J Am Chem Soc* 1897;19:930–934.
41. Kocbek P, Baumgartner S, Kristl J. Preparation and evaluation of nanosuspensions for enhancing the dissolution of poorly

- soluble drugs. *Int J Pharm* 2006;312:179–186.
42. Lai F, Pini E, Angioni G, et al. Nanocrystals as tool to improve piroxicam dissolution rate in novel orally disintegrating tablets. *Eur J Pharm Biopharm* 2011;79:552–558.
  43. Mauludin R, Müller RH, Keck CM. Kinetic solubility and dissolution velocity of rutin nanocrystals. *Eur J Pharm Sci* 2009; 36:502–510.
  44. Patravale V, Date A, Kulkarni R. Nanosuspensions: a promising drug delivery strategy. *J Pharm Pharmacol* 2004;56: 827–840.
  45. Nutan MTH, Reddy IK. General principles of suspensions. In: Kulshreshtha AA, Singh ON, Wall GM, eds. *Pharmaceutical suspensions: from formulation development to manufacturer*. New York: Springer; 2009:39–66.